DOI: 10.17344/acsi.2019.5159 *Acta Chim. Slov.* **2019,** *66,* 944–949

Scientific paper

DNA Interaction, *in vitro* Antibacterial and Cytotoxic Activities of Ru(III) Heterochelates

Parag S. Karia, Pankaj A. Vekariya, Anshul P. Patidar, Darshana N. Kanthecha, Bhupesh S. Bhatt and Mohan N. Patel*

Department of Chemistry, Sardar Patel University, Vallabh Vidyanagar–388 120, Gujarat, India

** Corresponding author: E-mail: jeenen@gmail.com, bhupeshbhatt31@gmail.com*
*Phone number: (+912692) 226856*218*

Received: 04-10-2019

Abstract

Ruthenium(III) complexes [Ru(bphtpy)(PPh_3)Cl_3] (bphfpy = diphenylfuranylpyridine derivatives) were synthesized and characterized by LCMS, IR spectroscopy, elemental analysis and magnetic measurements. All the complexes were screened for their antibacterial activity in terms of minimum inhibitory concentration against two Gram-positive and three Gram-negative bacterial species. DNA binding study by absorption titration and viscosity measurement shows that complexes bind in an intercalating mode, which is also confirmed by molecular docking. All the complexes were also screened for the DNA nuclease property of pUC19 plasmid DNA. The cytotoxicity study of the synthesized complexes was performed to elucidate the LC_{50} values to find out the toxicity profile of the complexes.

Keywords: N,O-donor ligand; Ruthenium(III)complexes; DNA interaction; Cytotoxicity

1. Introduction

A great history of transition metal complexes is associated with their effectiveness in the numerous diseases cure,[1–3] including the major application in the field of novel anticancer drug discovery. The interaction of coordination compounds with various biomolecules is facilitated due to varying oxidation states of central metal ion, which can eventually result in surprising pharmacological and exceptional curative properties.[4–8] Metals can alter the physiological condition and the intrinsic toxicity of metal ions can be reduced by their coordination with ligands. The biological properties of ligands can increase with metal chelation and can cause a synergistic effect on both ligand and metal ion.[10] Recently large interest has been drawn on the ruthenium based coordination compounds in anticancer drug development.[11–13]

Ruthenium can be seen as a promising metal after platinum due to its kinetics and timescales comparison to cellular division processes similar to platinum.[14] Ruthenium complexes with N,N-donor ligand have found significant application as metallo-intercalators.[15,16] Changing substituent groups in the ligand can create electron density distribution and space configuration differences of complexes, resulting in diverse spectral properties and biological activities.[17,18] The N,O–donor ligand has been selected owing to its antifungal activity exhibited due to furan ring,[19] and the role of bulky co-ligand is to stabilize the complex which prevents quick dissociation of the complex. hence the compound can reach the pharmacological target such as DNA.[20]

Keeping these aspects in mind, we synthesized of ruthenium(III) complexes with PPh_3 and N,O-donor ligand, and studied the antimicrobial activity, DNA interaction study and cytotoxic activity.

2. Experimental

Material and reagents: The analytical grade chemicals purchased were used as such without further purification. $RuCl_3{\cdot}3H_2O$, 4-chlorobenzaldehyde, 2-acetylfuran, 4-fluorobenzaldehyde, 4-bromobenzaldehyde, 3-chlorobenzaldehye, 3-fluorobenzaldehyde, 3-bromobenzaldehyde and HS-DNA were purchased from Sigma Chemical Co., India. Bromophenol blue, ethidium bromide (EB), Luria Broth and agarose were purchased from Himedia, India. Perkin–Elmer 240 Elemental Analyzer was used to collect microanalytical data. Room temperature magnetic susceptibility was measured by Gouy's method. FT–IR

data were collected by FT–IR ABB Bomen MB 3000 spectrophotometer. The ^{1}H NMR and ^{13}C NMR were recorded on a Bruker Avance (400 MHz). UV–Vis spectra of the complexes were recorded on UV-160A UV–Vis spectrophotometer, Shimadzu (Japan). Cleavage of pUC19 DNA was quantified by AlphaDigiDoc^{TM} RT. Version V.4.0.0. The thermogram of complexes were recorded with a Mettler Toledo TGA/DSC 1 thermogravimetric analyser.

Synthesis of ligands: The ligands (**L^1**–**L^6**) were synthesized according to the reported method using modified Krohnke pyridine synthesis method.[21] The synthesis and characterization of ligands are provided in the supplementary material.

Synthesis of Ru(III) complexes (1–6): $[RuCl_3(PPh_3)_3]$ was prepared by refluxing methanolic solution (50 mL) of $RuCl_3{\cdot}3H_2O$ (0.01 mol) with PPh_3 (0.03 mol) and conc. HCl (60 mL) for 1 h. The obtained reddish brown precipitates were filtered, dried and recrystallized by using hot methanol.

Synthesis of [Ru(L^1)(PPh$_3$)Cl$_3$] ***(1)****:* $[RuCl_3(PPh_3)_3]$ (0.1 mmol) in toluene (20 mL) and a methanolic solution (20 mL) of 4-(4-fluorophenyl)-2-(furan-2-yl)-6-*p*-tolylpyridine **(L^1)** (0.1 mmol) were combined and refluxed for 4 h. (Scheme 1). The blackish brown product obtained was washed with toluene to remove unreacted precursor and next washed with methanol to remove unreacted ligand and dried under vacuum. Yield: 22 %, m.p.: 287–290 °C, μ_{eff}: 1.89 B.M. Anal. Calc. for: $C_{40}H_{31}Cl_3FNOPRu$ (799.08): Calc. (%): C, 60.12; H, 3.91; N, 1.75; Ru, 12.65. Found (%): C, 60.03; H, 3.93; N, 1.70, $Ru_{(gravimetrically)}$, 12.60. IR (KBr, 4000–400 cm^{-1}): 3030, υ(C–H)ar stretching; 1545, υ(C=C); 1505, υ(C=N); 543, υ(Ru-O); 445, υ(Ru-N); 1454, 1032, 698, υ(PPh_3). UV–Vis. λ_{max} (nm) (DMSO): 560, 420, 260, Mass (*m*/*z*%): 800.06 (100) [M$^+$].

Synthesis of [Ru(L^2)(PPh$_3$)Cl$_3$] ***(2)****:* $[RuCl_3(PPh_3)_3]$ (0.1 mmol) in toluene (20 mL) and a methanolic solution (20 mL) of 4-(4-chlorophenyl)-2-(furan-2-yl)-6-*p*-tolylpyridine **(L^2)** (0.1 mmol) were combined and refluxed for 4 h. (Scheme 1). The blackish brown product obtained was washed with toluene to remove unreacted precursor and next washed with methanol to remove unreacted ligand and dried under vacuum. Yield: 19.9%, m.p.: 274-276 °C, μ_{eff}: 1.81 B.M. Anal. Calc. for: $C_{40}H_{31}Cl_4NOPRu$ (815.54): Calc. (%): C, 58.91; H, 3.83; N, 1.72; Ru, 12.39. Found (%): C, 58.84; H, 3.89; N, 1.78, $Ru_{(gravimetrically)}$, 12.37. IR (KBr, 4000–400 cm^{-1}): 3038, υ(C–H)ar stretching; 1541, υ(C=C); 1509, υ(C=N); 561, υ(Ru-O); 456, υ(Ru-N); 1458, 1029, 689, υ(PPh_3). UV–Vis. λ_{max}(nm) (In DMSO): 565, 425, 261.

Synthesis of [Ru(L^3)(PPh$_3$)Cl$_3$] ***(3)****:* $[RuCl_3(PPh_3)_3]$ (0.1 mmol) in toluene (20 mL) and a methanolic solution (20 mL) of 4-(4-bromophenyl)-2-(furan-2-yl)-6-*p*-tolylpyridine **(L^3)** (0.1 mmol) were combined and refluxed for 4 h. (Scheme 1). The dark brown product obtained was washed with toluene to remove unreacted precursor and next washed with methanol to remove unreacted ligand and dried under vacuum. Yield: 20.1%, m.p. >300 °C, μ_{eff}: 1.84 B.M. Anal. Calc. for: $C_{40}H_{31}Cl_3BrNOPRu$ (859.99): Calc. (%): C, 55.86; H, 3.63; N, 1.63; Ru, 11.75. Found (%): C, 55.78; H, 3.64; N, 1.66, $Ru_{(gravimetrically)}$, 11.79. IR (KBr, 4000–400 cm^{-1}): 3041, υ(C–H)ar stretching; 1541, υ(C=C); 1506, υ(C=N); 554, υ(Ru-O); 449, υ(Ru-N); 1462, 1029, 694, υ(PPh_3). UV–Vis. λ_{max}(nm) (In DMSO): 575, 430, 263.

Synthesis of [Ru(L^4)(PPh$_3$)Cl$_3$] ***(4)****:* $[RuCl_3(PPh_3)_3]$ (0.1 mmol) in toluene (20 mL) and a methanolic solution (20 mL) of 4-(3-fluorophenyl)-2-(furan-2-yl)-6-*p*-tolylpyridine **(L^4)** (0.1 mmol) were combined and refluxed for 4 h. (Scheme 1). The blackish brown product obtained was washed with toluene to remove unreacted precursor and next washed with methanol to remove unreacted ligand and dried under vacuum. Yield: 18.4%, m.p.: 286-290 °C, μ_{eff}: 1.86 B.M. Anal. Calc. for: $C_{40}H_{31}Cl_3FNOPRu$ (799.08): Calc. (%): C, 60.12; H, 3.91; N, 1.75; Ru, 12.65. Found (%): C, 60.13; H, 3.97; N, 1.68, $Ru_{(gravimetrically)}$, 12.72. IR (KBr, 4000–400 cm^{-1}): 3033, υ(C–H)ar stretching; 1549, υ(C=C); 1512, υ(C=N); 549, υ(Ru-O); 453, υ(Ru-N); 1456, 1021, 697, υ(PPh_3). UV–Vis. λ_{max}(nm) (In DMSO): 563, 420, 260.

Synthesis of [Ru(L^5)(PPh$_3$)Cl$_3$] ***(5)****:* $[RuCl_3(PPh_3)_3]$ (0.1 mmol) in toluene (20 mL) and a methanolic solution (20 mL) of 4-(3-chlorophenyl)-2-(furan-2-yl)-6-*p*-tolylpyridine **(L^5)** (0.1 mmol) were combined and refluxed for 4 h. (Scheme 1). The blackish brown product obtained was washed with toluene to remove unreacted precursor and next washed with methanol to remove unreacted ligand and dried under vacuum. Yield: 17%, m.p.: 276-278 °C, μ_{eff}: 1.80 B.M. Anal. Calc. for: $C_{40}H_{31}Cl_4NOPRu$ (815.54): Calc. (%): C, 58.91; H, 3.83; N, 1.72; Ru, 12.39. Found (%): C, 58.89; H, 3.79; N, 1.68, $Ru_{(gravimetrically)}$, 12.39. IR (KBr, 4000–400 cm^{-1}): 3054, υ(C–H)ar stretching; 1543, υ(C=C); 1507, υ(C=N); 563, υ(Ru-O); 446, υ(Ru-N); 1443, 1024, 692, υ(PPh_3). UV–Vis. λ_{max}(nm) (In DMSO): 570, 428, 262.

Synthesis of [Ru(PPh$_3$)(L^6)(Cl$_3$] ***(6)****:* $[RuCl_3(PPh_3)_3]$ (0.1 mmol) in toluene (20 mL) and a methanolic solution (20 mL) of 4-(3-bromophenyl)-2-(furan-2-yl)-6-*p*-tolylpyridine **(L^6)** (0.1 mmol) were combined and refluxed for 4 h. (Scheme 1). The dark brown product obtained was washed with toluene to remove unreacted precursor and next washed with methanol to remove unreacted ligand and dried under vacuum. Yield: 19%, m.p.: >300 °C, μ_{eff}: 1.89 B.M. Anal. Calc. for: $C_{40}H_{31}Cl_3BrNOPRu$ (859.99): Calc. (%): C, 55.86; H, 3.63; N, 1.63; Ru, 11.75. Found (%): C, 55.84; H, 3.60; N, 1.61, $Ru_{(gravimetrically)}$, 11.70. IR (KBr, 4000–400 cm^{-1}): 3063, υ(C–H)ar stretching; 1554, υ(C=C); 1510, υ(C=N); 546, υ(Ru-O); 460, υ(Ru-N); 1443, 1027, 690, υ(PPh_3). UV–Vis. λ_{max}(nm) (In DMSO): 571, 424, 262.

In vitro **antibacterial screening:** *In vitro* antibacterial study of all compounds was performed against three

Gram-negative and two Gram-positive bacteria according to the literature method.[22]

DNA interaction study: Metal–DNA interactions was probed using electronic absorption titration and viscosity measurement, according to the literature method.[23,24] The molecular docking study was performed by HEX 8.0 software.[25]

Cytotoxicity study: The Brine shrimp lethality activity (BSLA) test was carried out referring to the protocol of Mayer *et al.*[22]

Gel electrophoresis study: The DNA cleavage study for synthesized complexes was performed using the reported procedure.[26]

3. Results and Discussion

Synthesis: The N,O-donor ligands (**L^1–L^6**) were synthesized by refluxing the mixture of pyridinium salt of 2-acetylfuran and substituted enones in methanol in presence of excess of ammonium acetate for 6 h. The methanolic solution of the ligands and solution of ruthenium precursor $[RuCl_3(PPh_3)_3]$ in toluene were refluxed for 4 h to obtain complexes **1–6**. General reaction scheme for the synthesis of complexes is given in Scheme 1.

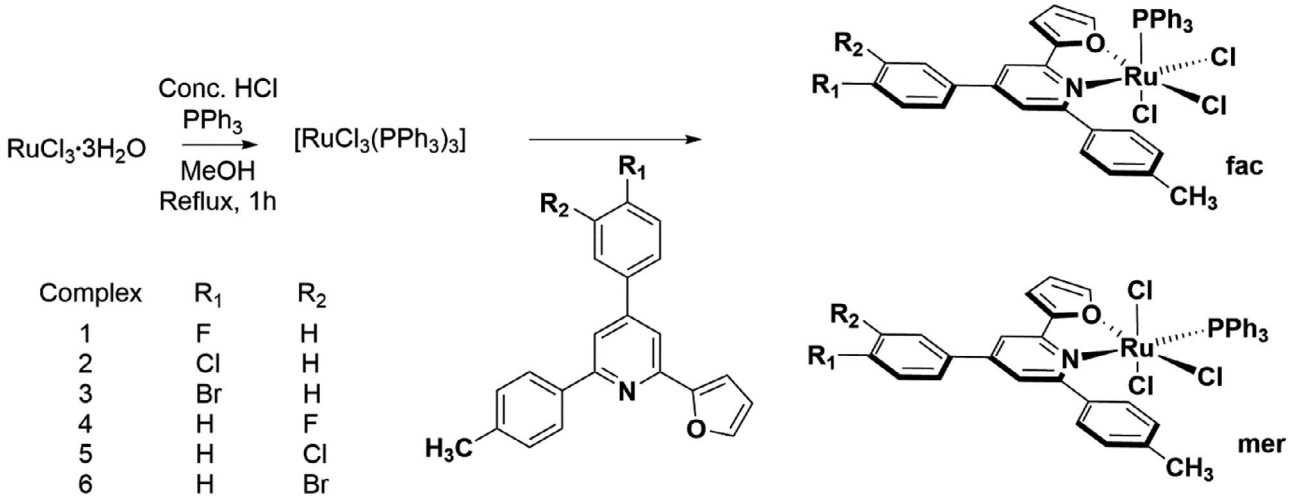

Complex	R_1	R_2
1	F	H
2	Cl	H
3	Br	H
4	H	F
5	H	Cl
6	H	Br

Scheme 1. Synthesis of ruthenium(III) complexes.

Spectral and analytical characterization: The electronic spectra showed three bands in the 260–575 nm region. The bands at 560–575 nm, 420–430 nm, 260 nm region corresponds to d–d transition, metal-to-ligand charge transfer and intraligand charge transfer, respectively. The magnetic moment of Ru(III) complexes was measured using Gouy's magnetic balance at room temperature. The magnetic moment values were found in the range of 1.80–1.89 BM. The theoretical spin-only value is 1.73 BM, which suggests that the metal ion in complexes possess one unpaired electron and possess ***s = ½ system.***

The thermogravimetric curve of complex **1** (Supplementary material) shows no mass loss up to 180 °C signifying the absence of water molecule or any volatile component. First mass loss (13.34%) during 190–260 °C corresponds to the loss of chlorine atoms. Second mass loss (32.72%) during 360–520 °C corresponds to the loss of PPh_3 moiety. The third mass loss (41.14%) during 610–810 °C corresponds to the loss of neutral bidentate ligand and leaving behind residual metal oxide.

Mass spectrum of complex **1** shows molecular ion peak at m/z = 800.06 (M), 802.06 (M+2), 804.07 (M+4) and 806.06 (M+6) (Supplementary material), due to the presence of covalently bonded three chlorine atoms (with metal ion). The peak observed at m/z = 763.09 corresponds to the one Cl atom loss. Other fragments observed are 728.09, 693.12, 470.91, 435.07, 431.07, 398.97, 364.07, 329.08 and 262.11 m/z, for which proposed fragmentation pattern is shown in supplementary material.

IR spectral data of ligands and complexes were compared (Supplementary material) to investigate the coordination of ligand with ruthenium ion. The ring stretching frequencies of ν(C=N) of ligands (1497–1487 cm^{-1})[27,28] were shifted to higher frequencies (1505–1512 cm^{-1}) in metal complex, suggests the metal ion coordination with the nitrogen atoms of heterocycles.[29] The $\nu(C{=}C)_{ar}$ and $\nu(C{-}H)_{ar.}$ bands were observed at 1541–1554 cm^{-1} and 3030–3063 cm^{-1}, respectively. Additional bands in metal complexes were observed at 543–563 cm^{-1} and 445–460 cm^{-1} corresponds to ν(Ru–O) and ν(Ru–N), respectively.[30,31]

***In vitro* antibacterial activity:** The antibiotics resistance among bacteria has become a global problem, which has risen the need of novel antimicrobial agents. The results

(Supplementary material) of antibacterial screening shows higher efficiency of ruthenium complexes than the parent ligands and ruthenium salt against tested bacterial species under identical experimental conditions. However, the synthesized complexes show lower antibacterial potency compared to standard antibiotic like ofloxacin (MIC = 1.24–2.0 μM, for different bacterial species under investigation). The increase in lipophilic nature due to chelation may be the reason for the potentiation of antibacterial activity of complexes. The different molecular targets of antibacterial agents for exerting their mode of action are cell wall synthesis and cytoplasmic membrane. The chelation increases the ability of a complex to cross a cell membrane[32] according to the Tweedy's chelation theory,[33] by decreasing the polarity of metal ion through partial sharing of positive charge over chelating atoms.

DNA interaction study: *Absorption titration:* The observed absorbance is plotted against wavelength and shift in absorbance and change in wavelength is calculated to investigate the binding mode. In the absorption spectra of $[Ru(L^1)(PPh_3)Cl_3]$ (Figure 1), it is found that upon increasing the DNA concentration, hypochromism is observed in MLCT (around 420 nm) and intra-ligand charge transfer bands (around 260 nm) with slightly red shift indicative of the intercalative mode of binding. The strength of binding is measured from K_b values obtained using the equation

$$[DNA]/(\varepsilon_a - \varepsilon_f) = [DNA]/(\varepsilon_b - \varepsilon_f) + 1/K_b(\varepsilon_b - \varepsilon_f)$$

where ε_a, ε_f, and ε_b correspond to A_{obsd}/[complex], the extinction coefficient of free complex, and complex in the fully bound form, respectively. The K_b values for complexes **1–6** are found 5.18×10^5, 3.41×10^5, 1.69×10^5, 1.66×10^5, 1.46×10^5 and 1.78×10^5 M^{-1}, respectively. The observed results show that complex **1** has the highest binding propensity with DNA, which can be attributed to the presence of most electronegative F atom as a substituent atom at *p*-position to the ancillary ligand. The trend is also followed for complex **2** and complex **3**, having Cl and Br atom as substituent atom at *p*-position to the ancillary ligand. The other complexes having ligand with halogen substituent at *m*-position have a relatively lower binding propensity. So we can say that the DNA binding affinity of complexes depends upon the electronic properties of ligands. The obtained K_b values of complexes are found higher than $[Ru(NH_3)_4(dip)]^{2+}$ (1.50×10^4 M^{-1}),[34] comparable to $[Ru(phen)_2pzip]^{2+}$ (9.5×10^5 M^{-1})[35] and lower than $[Ru(bpy)_2(HBT)]^{2+}$ (5.71×10^7 M^{-1}).[36] The absorption spectral data and plots of $[DNA]/(\varepsilon_a - \varepsilon_f)$ versus [DNA] for the titration of DNA with complexes **1–6** are shown in supplementary material.

Viscosity measurement: The viscosity of HS–DNA was measured by varying the concentration of the complexes, to further explore the interaction between ruthenium(III) complexes and DNA. The relative viscosity of the HS–DNA increases with complex solution addition (Supplementary material), suggesting intercalative mode of binding. The curve of complex **1** resembles very similar to EtBr and is much higher in magnitude than other complexes suggesting a strong interactive binding of complex **1** than other synthesized complexes.

Molecular docking study: To explore the interaction mode and binding affinity, docking studies were performed. The binding interaction of Ru(III) complexes (Figure 2) with duplex DNA sequence $d(ACCGACGTCGGT)_2$ was performed to explore the DNA binding site and complex-DNA helix orientation. Molecular docking study suggests preferentially intercalative mode of complex to DNA interaction, involving stacking interaction. The docked

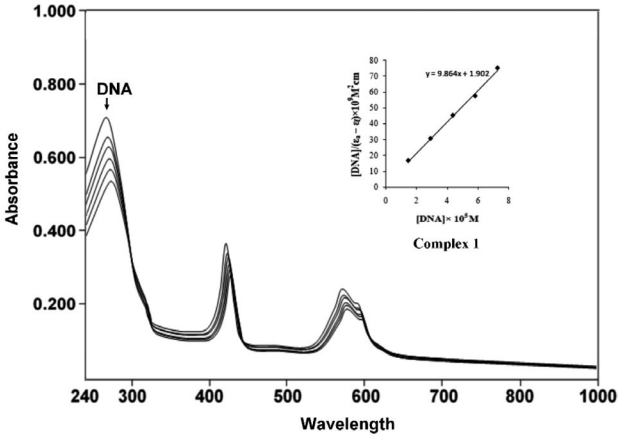

Figure 1. Electronic absorption spectra of complex **1** with increasing concentration of Herring Sperm DNA (HS–DNA) in phosphate buffer Inset: Plots of $[DNA]/(\varepsilon_a - \varepsilon_f)$ versus [DNA] for the titration of DNA with ruthenium(III) complex **1**.

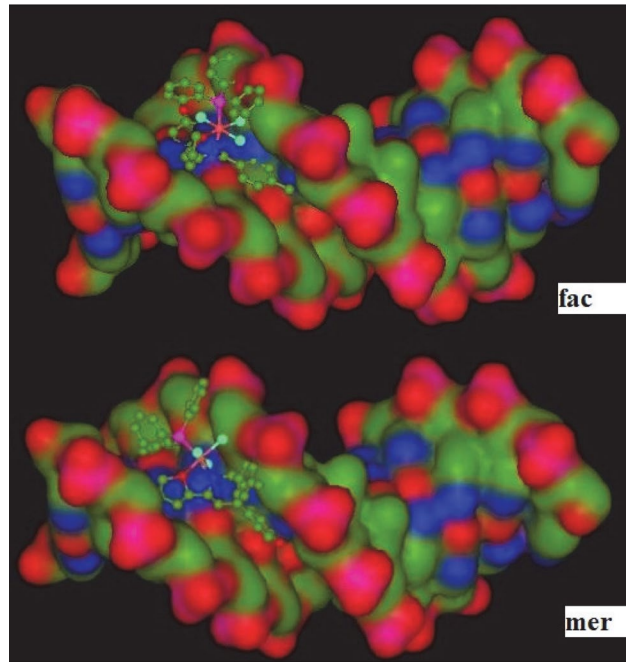

Figure 2. Molecular docking of the complex **1** (*fac* and *mer* isomers) with the DNA duplex.

structure showed the complexes fit well in between the stacks of rich A–T base pair region, which may be stabilized through hydrophobic or van der Waal's interaction. The binding energies of DNA-complexes interactions are –326.15, –326.58, –329.95, –325.63, –333.74, –329.94 kJ mol^{-1} for *fac*-complexes **1–6**, and –333.27, –338.44, –341.23, –343.46, –348.38, –339.77 kJ mol^{-1} for *mer*-complexes **1–6**, respectively.

Cytotoxicity: In this assay, the %mortality of brine shrimp nauplii was determined after 24 and 48 h of complexes treatment. The LC_{50} was evaluated from the plot of log[complex] against %mortality of nauplii. From the result, it is inferred that the complex **1** shows higher toxicity than other synthesized complexes and toxicity value (LC_{50} = 12.2, 14.1, 13.7, 12.9, 21.2 and 18.5 ***μM*** for complex **1–6**, respectively) of synthesized complexes are comparable to standard anticancer agent *cis*-platin (LC_{50} < 13.3 μM).

Gel electrophoresis study: Figure 3 shows the cleavage of DNA by the test compounds. Lane 1 is a control representing DNA cleavage into only two forms, supercoiled (Form I) and open circular (Form III). Lane 2 with the reference compound $RuCl_3{\cdot}2H_2O$ representing cleavage into only two forms similar to the control. Lane 3–8 contains synthesized ruthenium complexes **1–6** respectively, representing the cleavage of DNA into three forms Form I, Form III and Form II (linear) in between Form I and III generated by the scission of both the strands of DNA. The photographed image is quantified by AlphaDigiDoc software. The relative decrease in the supercoiled form of control after the addition of test compounds is a measure of percent cleavage. The results (Table 1) clearly indicate that

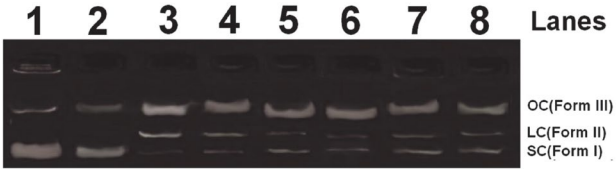

Figure 3. Cleavage of pUC19 plasmid DNA under the influence of ruthenium complexes. Lane 1, DNA control; Lane 2, $RuCl_3{\cdot}3H_2O$; Lane 3, $[Ru(L^1)(PPh_3)Cl_3]$; Lane 4, $[Ru(L^2)(PPh_3)Cl_3]$; Lane 5, $[Ru(L^3)(PPh_3)Cl_3]$; Lane 6, $[Ru(L^4)(PPh_3)Cl_3]$; Lane 7, $[Ru(L^5)(PPh_3)Cl_3]$; Lane 8, $[Ru(L^6)(PPh_3)Cl_3]$.

percent cleavage value is highest for the complex–**1** indicating its strong binding efficiency to DNA. The DNA cleavage data also follow the similar trend of binding constant value as measured by UV-visible absorption titration of metal complexes with increasing the concentration of DNA. So we can conclude that metal complex having higher DNA binding affinity can effectively cleave the DNA strand.

4. Conclusion

The data of various physicochemical activities like gravimetry, magnetic moment measurement and electronic spectral measurement are in good agreement with the proposed structure of metal complexes. The complexes have a paramagnetic nature. The MIC data suggest a significant increase in antibacterial activity of ligands after complexation with the metal ion. Also, that complexes **1–3** have comparatively higher antibacterial activity than complexes **4–6**. The MIC data clearly indicate that electronic properties (metal complexation and presence of F-substituent at *p*-position of L^1) play a vital role in enhancing the biological activities of complex **1** by increasing its lipophilic nature. Complex **1** binds more efficiently to the DNA via classical intercalation mode. The cytotoxic study displays good potency of the complexes against brine shrimp and 100% mortality is observed after 48 h of incubation. The efficient cleavage of supercoiled pUC19 DNA by all the complexes was observed. The higher efficacy of complex **1** in the various activity performed may be attributed to strong electron withdrawing potency of F-atom at the *para* position while and chlorine and bromine has less electron withdrawing capacity than bromine. This electron withdrawing capacity of fluorine atom makes the complex more polar and hence easily permeable to lipophilic layers of the target species and onset its action readily.

5. Acknowledgments

We are thankful to the Head, Department of Chemistry, Sardar Patel University; and UGC RFSMS Scheme for providing financial support.

Table 1. Gel electrophoresis analysis of complexes.

Lanes	Complexes	% OC	% LC	% SC	% Cleavage
1	Control	4.90	–	95.1	–
2	$RuCl_3{\cdot}3H_2O$	27.2	–	72.8	22.44
3	$[Ru(L^1)(PPh_3)Cl_3]$	68.2	24.0	7.80	91.79
4	$[Ru(L^2)(PPh_3)Cl_3]$	74.3	6.50	19.2	79.81
5	$[Ru(L^3)(PPh_3)Cl_3]$	73.3	9.00	17.7	81.39
6	$[Ru(L^4)(PPh_3)Cl_3]$	73.5	9.30	17.2	81.91
7	$[Ru(L^5)(PPh_3)Cl_3]$	58.7	5.20	36.0	62.14
8	$[Ru(L^6)(PPh_3)Cl_3]$	58.1	4.90	37.0	61.09

6. References

1. N. Farrell, Transition metal complexes as drugs and chemotherapeutic agents, Springer Science & Business Media, 2012.
2. U. Ndagi, N. Mhlongo, M. E. Soliman, *Drug Des. Devel. Ther.* **2017**, *11*, 599. **DOI:**10.2147/DDDT.S119488
3. S. J. S. Franchi, R. A. de Souza, A. E. Mauro, I. Z. Carlos, L. C. de Abreu Ribeiro, F. V. Rocha, A. V. de Godoy-Netto, *Acta Chim. Slov.* **2018**, *65*, 547–553. **DOI:**10.17344/acsi.2017.4112
4. R. S., *Biotech. Mol. Biol. Rev.* **2010**, *5*, 38.
5. N. Vamsikrishna, M. P. Kumar, G. Ramesh, N. Ganji, S. Daravath, *J. Chem. Sci.* **2017**, *129*, 609–622. **DOI:**10.1007/s12039-017-1273-7
6. B. B. Rajaretnam, J. Chellappa, D. A. Solomon, I. P. Subramanian, T. D. M. Selvanayagam, *Acta Chim. Slov.* **2019**.
7. M. Nišavić, R. Masnikosa, A. Butorac, K. Perica, A. Rilak, L. Korićanac, A. Hozić, M. Petković, M. Cindrić, *J. Inorg. Biochem.* **2016**, *159*, 89–95. **DOI:**10.1016/j.jinorgbio.2016.02.034
8. P. A. Vekariya, P. S. Karia, B. S. Bhatt, M. N. Patel, *Appl. Biochem. Biotech.* **2019**, *187*, 556–569. **DOI:**10.1007/s12010-018-2835-y
9. K. P. Thakor, M. V. Lunagariya, B. S. Bhatt, M. N. Patel, *Luminescence* **2019**, *34*, 113–124. **DOI:**10.1002/bio.3587
10. K. P. Thakor, M. V. Lunagariya, B. S. Bhatt, M. N. Patel, *Appl. Organomet. Chem.* **2018**, *32*, e4523. **DOI:**10.1002/aoc.4523
11. K. Lin, Z. Zhao, H. Bo, X. Hao, J. Wang, *Front. Pharmacol.* **2018**, *9*, 1323. **DOI:**10.3389/fphar.2018.01323
12. T. Lazarević, A. Rilak, Ž. D. Bugarčić, *Eur. J. Med. Chem.* **2017**, *142*, 8–31. **DOI:**10.1016/j.ejmech.2017.04.007
13. D. Lazić, A. Arsenijević, R. Puchta, Ž. D. Bugarčić, A. Rilak, *Dalton Trans.* **2016**, *45*, 4633–4646. **DOI:**10.1039/C5DT04132E
14. J. Reedijk, *Platin. Met. Rev.* **2008**, *52*, 2–11. **DOI:**10.1595/147106708X255987
15. J. K. Barton, A. Danishefsky, J. Goldberg, *J. Am. Chem. Soc.* **1984**, *106*, 2172–2176. **DOI:**10.1021/ja00319a043
16. J. Barton, *Science* **1986**, *233*, 727–734. **DOI:**10.1126/science.3016894
17. L.-F. Tan, X.-J. Chen, J.-L. Shen, X.-L. Liang, *J. Chem. Sci.* **2009**, *121*, 397–405. **DOI:**10.1007/s12039-009-0046-3
18. P. A. Vekariya, P. S. Karia, B. S. Bhatt, M. N. Patel, *J. Inorg. Organomet. Polym. Mater.* **2018**, *28*, 2749–2758. **DOI:**10.1007/s10904-018-0957-x
19. J.-Q. Huo, L.-Y. Ma, Z. Zhang, Z.-J. Fan, J.-L. Zhang, T. V. Beryozkina, V. A. Bakulev, *Chin. Chem. Lett.* **2016**, *27*, 1547–1550. **DOI:**10.1016/j.cclet.2016.06.019
20. S. Nadeem, M. Bolte, S. Ahmad, T. Fazeelat, S. A. Tirmizi, M. K. Rauf, S. A. Sattar, S. Siddiq, A. Hameed, S. Z. Haider, *Inorg. Chim. Acta* **2010**, *363*, 3261–3269. **DOI:**10.1016/j.ica.2010.06.015
21. F. KrÖHnke, *Synthesis* **1976**, *1976*, 1. **DOI:**10.1055/s-1976-23941
22. M. N. Patel, B. S. Bhatt, P. A. Dosi, *Inorg. Chem. Commun.* **2013**, *29*, 190–193. **DOI:**10.1016/j.inoche.2012.12.013
23. D. Lawrence, V. G. Vaidyanathan, B. U. Nair, *J. Inorg. Biochem.* **2006**, *100*, 1244–1251. **DOI:**10.1016/j.jinorgbio.2006.02.003
24. M. N. Patel, P. A. Dosi, B. S. Bhatt, *Acta Chim. Slov.* **2012**, *59*.
25. M.-L. Liu, M. Jiang, K. Zheng, Y.-T. Li, Z.-Y. Wu, C.-W. Yan, *J. Coord. Chem.* **2014**, *67*, 630–648. **DOI:**10.1080/00958972.2014.884218
26. M. N. Patel, P. A. Dosi, B. S. Bhatt, *Med. Chem. Res.* **2012**, *21*, 2723–2733. **DOI:**10.1007/s00044-011-9799-6
27. L.-W. Xue, H.-J. Zhang, P.-P. Wang, *Acta Chim. Slov.* **2019**, *66*, 190–195.
28. Y.-L. Sang, X.-S. Lin, *Acta Chim. Slov.* **2019**, *66*, 168–172.
29. P. R. Reddy, A. Shilpa, *Polyhedron* **2011**, *30*, 565–572. **DOI:**10.1016/j.poly.2010.11.015
30. G. G. Mohamed, E. M. Zayed, A. M. Hindy, *Spectrochim. Acta A* **2015**, *145*, 76–84. **DOI:**10.1016/j.saa.2015.01.129
31. A. S. Alturiqi, A.-N. Alaghaz, R. A. Ammar, M. E. Zayed, *J. Chem.* **2018**, *2018*. **DOI:**10.1155/2018/5816906
32. C. S. Allardyce, P. J. Dyson, D. J. Ellis, P. A. Salter, R. Scopelliti, *J. Organomet. Chem.* **2003**, *668*, 35–42. **DOI:**10.1016/S0022-328X(02)01926-5
33. B. Tweedy, *Phytopathology* **1964**, *55*, 910–914.
34. P. Uma Maheswari, M. Palaniandavar, *J. Inorg. Biochem.* **2004**, *98*, 219–230. **DOI:**10.1016/j.jinorgbio.2003.09.003
35. X.-W. Liu, J.-L. Lu, Y.-D. Chen, L. Li, D.-S. Zhang, *Inorg. Chim. Acta* **2011**, *379*, 1–6.
36. D. Lawrence Arockiasamy, S. Radhika, R. Parthasarathi, B. U. Nair, *Eur. J. Med. Chem.* **2009**, *44*, 2044–2051. **DOI:**10.1016/j.ejmech.2008.10.013

Povzetek

Sintetizirali smo rutenijeve(III) komplekse [Ru(bphtpy)(PPh_3)Cl_3] (bphfpy = derivati difenilfuranilpiridina) in jih okarakterizirali z LCMS, IR spektroskopijo, elementno analizo in magnetnimi meritvami. Vsem kompleksom smo določili antibakterijsko aktivnost z minimalno inhibitorno koncentracijo na dveh Gram pozitivnih in treh Gram negativnih bakterijskih vrstah. Študij vezave na DNA z absorptivno titracijo in viskozimetričnimi meritvami kaže, da se kompleksi vežejo na interkalacijski način, kar smo potrdili tudi z molekulskim dokingom. Vse komplekse smo tudi testirali za DNA nukleazne lastnosti na pUC19 plazmidski DNA. S citostatičnimi testi smo določili LC_{50} vrednosti z namenom določitve toksičnega profila kompleksov.